Domain wall motion in thin ferromagnetic nanotubes: Analytic results

2014 EPL 105 67006

(http://iopscience.iop.org/0295-5075/105/6/67006)

OPEN ACCESS

epl A LETTERS JOURNAL EXPLORING THE FRONTIERS OF PHYSICS

Made open access 29 December 2014

March 2014

EPL, **105** (2014) 67006
doi: 10.1209/0295-5075/105/67006

www.epljournal.org

Domain wall motion in thin ferromagnetic nanotubes: Analytic results

ARSENI GOUSSEV[1,2], J. M. ROBBINS[3] and VALERIY SLASTIKOV[3]

[1] *Department of Mathematics and Information Sciences, Northumbria University Newcastle Upon Tyne, NE1 8ST, UK*
[2] *Max Planck Institute for the Physics of Complex Systems - Nöthnitzer Straße 38, D-01187 Dresden, Germany*
[3] *School of Mathematics, University of Bristol - University Walk, Bristol, BS8 1TW, UK*

received 27 December 2013; accepted in final form 17 March 2014
published online 28 March 2014

PACS 75.75.-c – Magnetic properties of nanostructures
PACS 75.78.Fg – Dynamics of domain structures

Abstract – Dynamics of magnetization domain walls (DWs) in thin ferromagnetic nanotubes subject to weak longitudinal external fields is addressed analytically in the regimes of strong and weak penalization. Exact solutions for the DW profiles and formulas for the DW propagation velocity are derived in both regimes. In particular, the DW speed is shown to depend nonlinearly on the nanotube radius.

The problem of controlled manipulation of magnetization domains in quasi–one-dimensional ferromagnetic nanostructures is of paramount technological importance in designing new-generation memory devices [1–3] and of fundamental interest in the vibrant areas of micromagnetics and spintronics. To date, substantial theoretical progress has been achieved in understanding the dynamics of domain walls (DWs) in nanowires and nanostrips under the influence of applied magnetic fields [4–16] and spin-polarized electric currents [11,12,16–20]. Nevertheless, the search for schemes and regimes allowing fast and energy-efficient DW propagation actively continues.

Ferromagnetic nanotubes have been proposed as an alternative device geometry for carrying and manipulating DWs [21,22], and are attracting considerable attention not only for applications [23,24] but also from the point of view of basic theory and numerical simulations [25–30]. A key advantage of the nanotube structure is greater DW stability under strong fields [30] as compared to wire and strip geometries [4,31], leading to a significant increase in the DW velocity. A striking phenomenon is the dependence on chirality; with the central DW vortex oppositely oriented to the applied field, the DW motion exhibits a high-field Walker-like breakdown, whereas breakdown may be suppressed or even absent when the vortex is aligned with the applied field [26–28].

In this paper, we analytically address the DW dynamics in thin ferromagnetic nanotubes under the action of an

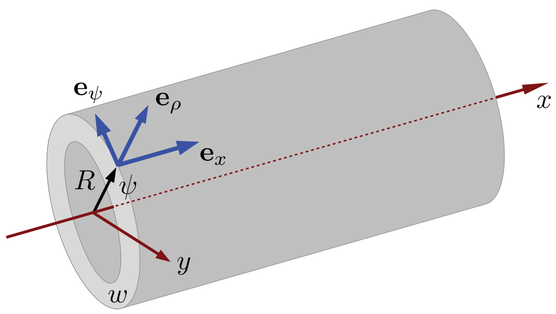

Fig. 1: (Colour on-line) A sketch of a nanotube with an outer radius R and an inner radius $R-w$. A point on the outer surface of the nanotube is parametrized by the coordinate x along its symmetry axis and the polar angle ψ. The unit vectors $\mathbf{e}_x$ (parallel to the symmetry axis), $\mathbf{e}_\psi$ (tangential to the surface), and $\mathbf{e}_\rho$ (normal to the surface) form a right-handed triplet.

external magnetic field and derive an explicit formula for the DW propagation speed in the regimes of strong and weak penalization. Our formula reveals a nonlinear dependence of the propagation speed on the nanotube radius, and may be used as a guide in devising new experiments.

We consider an infinitely long ferromagnetic nanotube with an outer radius R and an inner radius $(R-w)$ (see fig. 1). The magnetization distribution at a spatial point $\mathbf{x}$ and time t is described by $\mathbf{M}(\mathbf{x},t) = M_s\mathbf{m}(\mathbf{x},t)$, where $|\mathbf{m}(\mathbf{x},t)| = 1$ if $\mathbf{x} \in \Omega$ (the point belongs to the nanotube region) and $|\mathbf{m}(\mathbf{x},t)| = 0$ if $\mathbf{x} \notin \Omega$ (the point lies outside the nanotube region). Here, M_s stands for the saturation magnetization. The full micromagnetic energy of the nanotube is given by [32]

$$E(\mathbf{m}) = A\int_\Omega |\nabla \mathbf{m}|^2 \mathrm{d}\mathbf{x} + K\int_\Omega \left[1 - (\mathbf{m}\cdot\mathbf{e}_x)^2\right]\mathrm{d}\mathbf{x} + \frac{\mu_0 M_s^2}{2}\int_{\mathbb{R}^3} |\nabla u|^2 \mathrm{d}\mathbf{x}, \quad (1)$$

where the magnetostatic potential $u(\mathbf{x},t)$ satisfies

$$\nabla\cdot(\nabla u + \mathbf{m}) = 0 \quad \text{for} \quad \mathbf{x}\in\mathbb{R}^3. \quad (2)$$

Here, A denotes the exchange constant, K is the easy axis anisotropy constant, $\mu_0 = 4\pi\times 10^{-7}\,\mathrm{Wb}/(\mathrm{A}\cdot\mathrm{m})$ is the magnetic permeability of vacuum, and $\mathbf{e}_x$ is a unit vector pointing along the symmetry axis (x-axis) of the nanotube (see eq. (1)).

Within a continuum description, the time evolution of the magnetization distribution is governed by the Landau-Lifshitz (LL) equation [32]

$$\frac{\partial \mathbf{m}}{\partial t} = \gamma \mathbf{m}\times\mathbf{H} - \alpha \mathbf{m}\times(\mathbf{m}\times\mathbf{H}). \quad (3)$$

Here, γ denotes the gyromagnetic ratio, α is a phenomenological damping parameter, and $\mathbf{H}$ is an effective magnetic field, given by

$$\mathbf{H}(\mathbf{m}) = -\frac{1}{\mu_0 M_s}\frac{\delta E}{\delta \mathbf{m}} + \mathbf{H}_a, \quad (4)$$

where $\mathbf{H}_a$ stands for the applied (external) magnetic field. Being interested in the dynamics of a magnetization domain wall (DW), we focus on solutions of eq. (3) subject to the boundary conditions $\mathbf{m}(\mathbf{x},t)\to\pm\mathbf{e}_x$ for $x\to\pm\infty$ (and $\mathbf{x}\in\Omega$).

We now address the case of a thin nanotube, such that $w \ll R$. In this limit, the volume integrals in eq. (1) can be approximately reduced to integrals over the surface of a cylinder, and the stray-field energy can be approximated by an additional effective local anisotropy that penalises the magnetization component in the radial direction (see [33,34] for mathematical details of this procedure). Thus, rescaling the spatial variables, $\mathbf{x} = R\boldsymbol{\xi}$; the micromagnetic energy, $E = 2Aw\mathcal{E}$; and the effective and applied fields, $\mathbf{H} = [2A/(\mu_0 M_s R^2)]\boldsymbol{\mathcal{H}}$ and $\mathbf{H}_a = [2A/(\mu_0 M_s R^2)]\boldsymbol{\mathcal{H}}_a$, we approximate eqs. (1)–(4) by

$$\mathcal{E}(\mathbf{m}) = \frac{1}{2}\int_S |\nabla_S \mathbf{m}|^2 \mathrm{d}\sigma + \frac{\kappa}{2}\int_S \left[1-(\mathbf{m}\cdot\mathbf{e}_x)^2\right]\mathrm{d}\sigma + \frac{\lambda}{2}\int_S (\mathbf{m}\cdot\mathbf{e}_\rho)^2 \mathrm{d}\sigma \quad (5)$$

and

$$\boldsymbol{\mathcal{H}}(\mathbf{m}) = \nabla_S^2 \mathbf{m} + \kappa(\mathbf{m}\cdot\mathbf{e}_x)\mathbf{e}_x - \lambda(\mathbf{m}\cdot\mathbf{e}_\rho)\mathbf{e}_\rho + \boldsymbol{\mathcal{H}}_a, \quad (6)$$

where $\kappa = KR^2/A$ and $\lambda = \mu_0 M_s^2 R^2/(2A)$. The integrals in eq. (5) run over the surface of an infinitely long cylinder of unit radius, and $\nabla_S = \mathbf{e}_x\frac{\partial}{\partial\xi} + \mathbf{e}_\psi\frac{\partial}{\partial\psi}$ represents the surface gradient (and, accordingly, $\nabla_S^2 = \frac{\partial^2}{\partial\xi^2} + \frac{\partial^2}{\partial\psi^2}$ the surface Laplacian). Consequently, rescaling the time variable as $t = [\mu_0 M_s R^2/(2\gamma A)]\tau$, we rewrite the LL equation (3) in the dimensionless form,

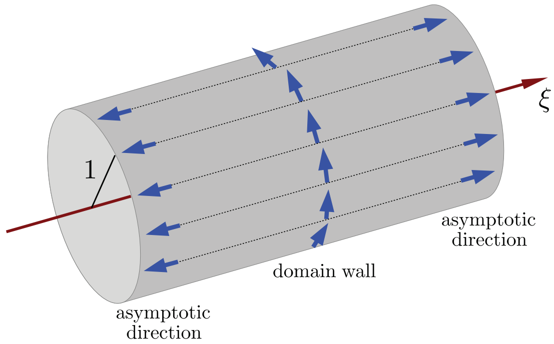

Fig. 2: (Colour on-line) A sketch of a magnetization DW for the case of $\lambda \gg 1$.

$$\frac{\partial \mathbf{m}}{\partial \tau} = \mathbf{m}\times\boldsymbol{\mathcal{H}} - \frac{\alpha}{\gamma}\mathbf{m}\times(\mathbf{m}\times\boldsymbol{\mathcal{H}}). \quad (7)$$

Equations (5)–(7), along with the boundary condition $\mathbf{m}(\xi,\tau)\to\pm\mathbf{e}_x$ as $\xi\to\pm\infty$ specify the magnetization dynamics problem addressed in this paper. Throughout we consider the regime $\kappa = O(1)$, which corresponds to nanotube radii R comparable to the exchange length $\sqrt{A/K}$. Below we consider the two limiting cases $\lambda \gg 1$ and $\lambda \ll 1$, which correspond to $K \ll \mu_0 M_s^2$ (weak anisotropy) and $K \gg \mu_0 M_s^2$ (strong anisotropy), respectively. In both cases we provide exact, traveling-wave solutions of the LL equation.

Strong-penalization case, $\lambda \gg 1$. In ferromagnetic nanotubes with very large λ and applied fields of order 1, the penalization term in the micromagnetic energy, eq. (5), essentially forces the magnetization distribution $\mathbf{m}$ to lie nearly tangent to the cylinder (see fig. 2). More specifically, it can be shown that $\mathbf{m} = \mathbf{m}_t + \lambda^{-1}\mathbf{m}_n$, where $\mathbf{m}_t = (\mathbf{m}\cdot\mathbf{e}_x)\mathbf{e}_x + (\mathbf{m}\cdot\mathbf{e}_\psi)\mathbf{e}_\psi$ is tangent to the cylinder and $\mathbf{m}_n = (\mathbf{m}\cdot\mathbf{e}_\rho)\mathbf{e}_\rho$ (with $|\mathbf{m}_n| \sim \mathcal{O}(1)$) is normal to the cylinder surface.

Resolving the effective field into its tangential and normal components $\boldsymbol{\mathcal{H}}_t = (\boldsymbol{\mathcal{H}}\cdot\mathbf{e}_x)\mathbf{e}_x + (\boldsymbol{\mathcal{H}}\cdot\mathbf{e}_\psi)\mathbf{e}_\psi$ and $\boldsymbol{\mathcal{H}}_n = (\boldsymbol{\mathcal{H}}\cdot\mathbf{e}_\rho)\mathbf{e}_\rho$ (both $|\boldsymbol{\mathcal{H}}_t|$ and $|\boldsymbol{\mathcal{H}}_n|$ being of order 1), we rewrite eq. (7) as $\frac{\mathrm{d}}{\mathrm{d}\tau}\mathbf{m}_t = \mathbf{m}_t\times(\boldsymbol{\mathcal{H}}_t + \boldsymbol{\mathcal{H}}_n) - \frac{\alpha}{\gamma}\mathbf{m}_t\times[\mathbf{m}_t\times(\boldsymbol{\mathcal{H}}_t+\boldsymbol{\mathcal{H}}_n))] + \mathcal{O}(\lambda^{-1})$. Then, resolving this equation into its tangential and normal components and keeping terms of the leading order in λ^{-1}, we obtain

$$\frac{\mathrm{d}}{\mathrm{d}\tau}\mathbf{m}_t = \mathbf{m}_t\times\boldsymbol{\mathcal{H}}_n - \frac{\alpha}{\gamma}\mathbf{m}_t\times(\mathbf{m}_t\times\boldsymbol{\mathcal{H}}_t), \quad (8)$$

$$0 = \mathbf{m}_t\times\boldsymbol{\mathcal{H}}_t - \frac{\alpha}{\gamma}\mathbf{m}_t\times(\mathbf{m}_t\times\boldsymbol{\mathcal{H}}_n). \quad (9)$$

Taking the cross product of both sides of eq. (9) with $\mathbf{m}_t$, and using $|\mathbf{m}_t|^2 = 1 + O(\lambda^{-2})$ we obtain, to the leading order in λ^{-1},

$$\mathbf{m}_\mathrm{t} \times \boldsymbol{\mathcal{H}}_\mathrm{n} = -\frac{\gamma}{\alpha}\mathbf{m}_\mathrm{t} \times (\mathbf{m}_\mathrm{t} \times \boldsymbol{\mathcal{H}}_\mathrm{t}). \tag{10}$$

Finally, substituting eq. (10) into eq. (8), we conclude that, in the limit $\lambda \to \infty$ (or, more generally, in the leading order in λ^{-1}) the time evolution of $\mathbf{m}(\xi, \psi, \tau)$ is governed by the modified LL equation,

$$\frac{\partial \mathbf{m}}{\partial \tau} = -\left(\frac{\alpha}{\gamma} + \frac{\gamma}{\alpha}\right)\mathbf{m} \times (\mathbf{m} \times \boldsymbol{\mathcal{H}}_\mathrm{t}), \tag{11}$$

where the magnetization distribution is restricted to be tangent to the surface of the cylinder,

$$\mathbf{m} = \mathbf{e}_x \cos\theta + \mathbf{e}_\psi \sin\theta. \tag{12}$$

In general, $\theta = \theta(\xi, \psi, \tau)$. A similar result has been obtained for the effective dynamics in thin ferromagnetic films [35].

We now assume that the applied magnetic field is directed along the nanotube axis, $\boldsymbol{\mathcal{H}}_\mathrm{a} = \mathcal{H}_\mathrm{a}\mathbf{e}_x$. Substituting eq. (12) into eq. (6), taking into account the fact that $\frac{\partial}{\partial\psi}\mathbf{e}_\psi = -\mathbf{e}_\rho$ and $\frac{\partial}{\partial\psi}\mathbf{e}_\rho = \mathbf{e}_\psi$, and discarding the component of $\boldsymbol{\mathcal{H}}$ along $\mathbf{e}_\rho$, we obtain the tangential component of the effective field,

$$\begin{aligned}\boldsymbol{\mathcal{H}}_\mathrm{t} = {}& \big(-\sin\theta\nabla_S^2\theta - \cos\theta|\nabla_S\theta|^2 + \kappa\cos\theta + \mathcal{H}_\mathrm{a}\big)\mathbf{e}_x \\ &+ \big(\cos\theta\nabla_S^2\theta - \sin\theta|\nabla_S\theta|^2 - \sin\theta\big)\mathbf{e}_\psi.\end{aligned} \tag{13}$$

Consequently,

$$\begin{aligned}&\mathbf{m} \times (\mathbf{m} \times \boldsymbol{\mathcal{H}}_\mathrm{t}) = \\ &\big(\nabla_S^2\theta - (1+\kappa)\sin\theta\cos\theta - \mathcal{H}_\mathrm{a}\sin\theta\big)(\mathbf{e}_x\sin\theta - \mathbf{e}_\psi\cos\theta).\end{aligned} \tag{14}$$

Thus, using the identity $\frac{\partial}{\partial\tau}\mathbf{m} = -(\mathbf{e}_x\sin\theta - \mathbf{e}_\psi\cos\theta)\frac{\partial}{\partial\tau}\theta$ and eq. (14) in the left- and right-hand side of eq. (11) respectively, we obtain

$$\frac{\partial\theta}{\partial\tau} = \left(\frac{\alpha}{\gamma} + \frac{\gamma}{\alpha}\right)\big(\nabla_S^2\theta - (1+\kappa)\sin\theta\cos\theta - \mathcal{H}_\mathrm{a}\sin\theta\big). \tag{15}$$

Equation (15) governs the dynamics of the magnetization distribution, given by eq. (12), subject to the boundary conditions $\lim_{\xi\to-\infty}\theta(\xi,\psi,\tau) = \pi$ and $\lim_{\xi\to+\infty}\theta(\xi,\psi,\tau) = 0$. It can be straightforwardly verified that this problem admits a family of exact traveling-wave solutions

$$\theta(\xi,\psi,\tau) = \Theta_1\big(\xi - \xi_0(\tau)\big), \tag{16}$$

where the function

$$\Theta_1(\xi) = 2\tan^{-1}\exp\left(-\xi\sqrt{1+\kappa}\right) \tag{17}$$

(or, equivalently, $\frac{\mathrm{d}}{\mathrm{d}\xi}\Theta_1 = -\sqrt{1+\kappa}\sin\Theta_1$) determines the spatial profile of the traveling wave, and

$$\frac{\mathrm{d}\xi_0}{\mathrm{d}\tau} = -\left(\frac{\alpha}{\gamma} + \frac{\gamma}{\alpha}\right)\frac{\mathcal{H}_\mathrm{a}}{\sqrt{1+\kappa}} \tag{18}$$

gives the propagation velocity. In the original physical coordinates, the propagation velocity reads

$$\frac{\mathrm{d}x_0}{\mathrm{d}t} = -\left(\frac{\alpha}{\gamma} + \frac{\gamma}{\alpha}\right)\frac{\gamma R H_a}{\sqrt{1 + KR^2/A}}. \tag{19}$$

Equation (19) gives explicitly the nonlinear dependence of the DW propagation speed on the nanotube radius. Thus, in the anisotropic case ($K > 0$), our formula shows that $|\frac{\mathrm{d}}{\mathrm{d}t}x_0| \propto RH_\mathrm{a}$ for $R \ll \sqrt{A/K}$, and $|\frac{\mathrm{d}}{\mathrm{d}t}x_0| \propto H_\mathrm{a}$ for $R \gg \sqrt{A/K}$. In the isotropic case ($K = 0$), however, $|\frac{\mathrm{d}}{\mathrm{d}t}x_0| \propto RH_\mathrm{a}$ at any nanotube radius.

Weak-penalization case, $\lambda \ll 1$. We now focus on the case of a strongly anisotropic ferromagnetic nanotube for which the penalization parameter λ is negligibly small. In this case the magnetization distribution $\mathbf{m}$ is no longer restricted to lie tangent to the cylinder and explores the full unit sphere. Its time evolution is governed by the LL equation (7) with the effective field approximated by (cf. eq. (6))

$$\boldsymbol{\mathcal{H}} = \nabla_S^2\mathbf{m} + (\kappa\mathbf{m}\cdot\mathbf{e}_x + \mathcal{H}_\mathrm{a})\mathbf{e}_x. \tag{20}$$

Substituting the Cartesian representation of the magnetization distribution, $\mathbf{m} = (\cos\theta, \sin\theta\cos\phi, \sin\theta\sin\phi)$, into eqs. (7) and (20), we obtain a system of two coupled nonlinear PDEs for the unknown functions $\theta = \theta(\xi,\psi,\tau)$ and $\phi = \phi(\xi,\psi,\tau)$:

$$\frac{\partial\theta}{\partial\tau} + \frac{\gamma}{\alpha}\frac{\partial\phi}{\partial\tau}\sin\theta = \left(\frac{\alpha}{\gamma} + \frac{\gamma}{\alpha}\right)\mathcal{F}_1, \tag{21}$$

$$-\frac{\gamma}{\alpha}\frac{\partial\theta}{\partial\tau} + \frac{\partial\phi}{\partial\tau}\sin\theta = \left(\frac{\alpha}{\gamma} + \frac{\gamma}{\alpha}\right)\mathcal{F}_2, \tag{22}$$

where

$$\begin{aligned}\mathcal{F}_1 = {}& \frac{\partial^2\theta}{\partial\xi^2} + \frac{\partial^2\theta}{\partial\psi^2} - \left[\kappa + \left(\frac{\partial\phi}{\partial\xi}\right)^2 + \left(\frac{\partial\phi}{\partial\psi}\right)^2\right]\sin\theta\cos\theta \\ &- \mathcal{H}_\mathrm{a}\sin\theta,\end{aligned} \tag{23}$$

$$\mathcal{F}_2 = 2\left[\frac{\partial\theta}{\partial\xi}\frac{\partial\phi}{\partial\xi} + \frac{\partial\theta}{\partial\psi}\frac{\partial\phi}{\partial\psi}\right]\cos\theta + \left[\frac{\partial^2\phi}{\partial\xi^2} + \frac{\partial^2\phi}{\partial\psi^2}\right]\sin\theta. \tag{24}$$

As before, this system is to be solved subject to the boundary conditions $\lim_{\xi\to-\infty}\theta(\xi,\psi,\tau) = \pi$ and $\lim_{\xi\to+\infty}\theta(\xi,\psi,\tau) = 0$.

As can be readily verified by a direct substitution, this problem admits a two-parameter family of exact traveling-wave solutions

$$\theta(\xi,\psi,\tau) = \Theta_n\big(\xi - \xi_0(\tau)\big), \tag{25}$$

$$\phi(\xi,\psi,\tau) = n\psi + \Phi(\tau), \tag{26}$$

with $n \in \mathbb{Z}$. Here, the longitudinal profile of the DW is given by

$$\Theta_n(\xi) = 2\tan^{-1}\exp\left(-\xi\sqrt{n^2+\kappa}\right) \tag{27}$$

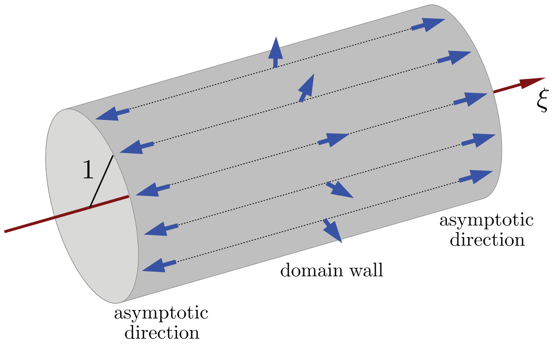

Fig. 3: (Colour on-line) A sketch of the magnetization DW for the case of $\lambda \ll 1$. The DW has the helicity index $n = 1$.

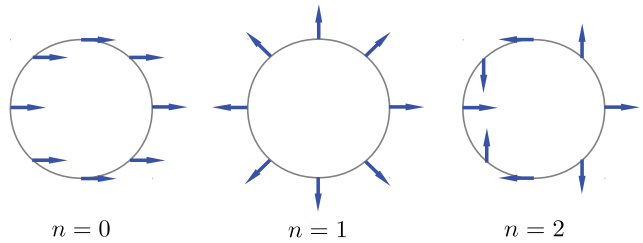

Fig. 4: (Colour on-line) Magnetization in a cross-section of the nanotube for different helicities n. The case $n = 0$ corresponds to a transverse domain wall [26].

(or, equivalently, $\frac{\mathrm{d}}{\mathrm{d}\xi}\Theta_n = -\sqrt{n^2+\kappa}\sin\Theta_n$), the precession velocity by

$$\frac{\mathrm{d}\Phi}{\mathrm{d}\tau} = -\mathcal{H}_\mathrm{a}, \tag{28}$$

and the propagation velocity by

$$\frac{\mathrm{d}\xi_0}{\mathrm{d}\tau} = -\frac{\alpha}{\gamma}\frac{\mathcal{H}_\mathrm{a}}{\sqrt{n^2+\kappa}}. \tag{29}$$

In the original physical coordinates, the propagation velocity reads

$$\frac{\mathrm{d}x_0}{\mathrm{d}t} = -\frac{\alpha R H_\mathrm{a}}{\sqrt{n^2+KR^2/A}}. \tag{30}$$

In eqs. (25)–(30), the index n measures the DW helicity. That is, n counts the number of times that the magnetization vector turns about $\mathbf{e}_x$ as the circumference of the cylinder is traversed. A sketch of a DW with $n = 1$ is shown in fig. 3, and cross-sections for different n are shown in fig. 4. It is interesting to note that DWs with lower helicity (and lower free energy) propagate faster. The maximal propagation speed $|\frac{\mathrm{d}}{\mathrm{d}\tau}\xi_0| = (\alpha/\gamma)|\mathcal{H}_\mathrm{a}|/\sqrt{\kappa}$ is achieved for $n = 0$ and is independent of R. As in the strong-penalization case (cf eq. (19)), eq. (30) gives the full nonlinear dependence of the DW propagation speed on the nanotube radius. We see that $|\frac{\mathrm{d}}{\mathrm{d}t}x_0| \propto RH_\mathrm{a}$ for $R \ll n\sqrt{A/K}$, while $|\frac{\mathrm{d}}{\mathrm{d}t}x_0| \propto H_\mathrm{a}$ for $R \gg n\sqrt{A/K}$.

In conclusion, we have conducted an analytic study of the DW dynamics in thin ferromagnetic nanotubes subject to external longitudinal magnetic fields. We have found explicit functional forms of the DW profiles and derived explicit formulas for the DW velocity in the regimes of strong and weak penalization, eqs. (19) and (30), respectively. In the strong-penalization case, the magnetization field lies nearly tangent to the nanotube, while for weak penalizations, the magnetization vector may wrap around the nanotube with any integer helicity index. The DW propagation speed increases with the nanotube radius in a nonlinear way, and, in the weak-penalization case, decreases with increasing helicity. Since for a typical ferromagnetic material $\alpha/\gamma \ll 1$, DWs in the strong-penalization case propagate much faster than those in the weak-penalization case. It would be of considerable interest to extend this analysis to the intermediate regime, where chirality-dependent breakdown phenomena have been observed, and the DW profile is known to depend on the applied field. In accord with previous studies, we would expect the finite width of the nanotube to play a role.

* * *

AG thanks EPSRC for support under grant EP/K024116/1, JMR thanks EPSRC for support under grant EP/K02390X/1, and VS thanks EPSRC for support under grants EP/I028714/1 and EP/K02390X/1.

REFERENCES

[1] Parkin S. S. P., Hayashi M. and Thomas L., *Science*, **320** (2008) 190.
[2] Hayashi M., Thomas L., Moriya R., Rettner C. and Parkin S. S. P., *Science*, **320** (2008) 209.
[3] Thomas L., Moriya R., Rettner C. and Parkin S. S. P., *Science*, **330** (2010) 1810.
[4] Schryer N. L. and Walker L. R., *J. Appl. Phys.*, **45** (1974) 5406.
[5] Tatara G. and Kohno H., *Phys. Rev. Lett.*, **92** (2004) 086601.
[6] Beach G. S. S., Nistor C., Knutson C., Tsoi M. and Erskine J. L., *Nat. Mater.*, **4** (2005) 741.
[7] Mougin A., Cormier M., Adam J. P., Metaxas P. J. and Ferré J., *EPL*, **78** (2007) 57007.
[8] Tretiakov O. A., Clarke D., Chern G.-W., Bazaliy Y. B. and Tchernyshyov O., *Phys. Rev. Lett.*, **100** (2008) 127204.
[9] Bryan M. T., Schrefl T., Atkinson D. and Allwood D. A., *J. Appl. Phys.*, **103** (2008) 073906.
[10] Wang X. R., Yan P. and Lu J., *EPL*, **86** (2009) 67001.
[11] Tretiakov O. A. and Abanov Ar., *Phys. Rev. Lett.*, **105** (2010) 157201.
[12] Tretiakov O. A., Liu Y. and Abanov Ar., *Phys. Rev. Lett.*, **108** (2012) 247201.
[13] Sun Z. Z. and Schliemann J., *Phys. Rev. Lett.*, **104** (2010) 037206.
[14] Goussev A., Robbins J. M. and Slastikov V., *Phys. Rev. Lett.*, **104** (2010) 147202.

[15] Goussev A., Lund R. G., Robbins J. M., Slastikov V. and Sonnenberg C., *Phys. Rev. B*, **88** (2013) 024425.
[16] Goussev A., Lund R. G., Robbins J. M., Slastikov V. and Sonnenberg C., *Proc. R. Soc. A*, **469** (2013) 20130308.
[17] Berger L., *Phys. Rev. B*, **54** (1996) 9353.
[18] Slonczewski J. C., *J. Magn. & Magn. Mater.*, **159** (1996) L1.
[19] Thiaville A., Nakatani Y., Miltat J. and Suzuki Y., *EPL*, **69** (2005) 990.
[20] Yan M., Kákay A., Gliga S. and Hertel R., *Phys. Rev. Lett.*, **104** (2010) 057201.
[21] Wang Z. K. *et al.*, *Phys. Rev. Lett.*, **94** (2005) 137208.
[22] Kläui M. *et al.*, *Phys. Rev. Lett.*, **94** (2005) 106601.
[23] Rüffer D. *et al.*, *Nanoscale*, **4** (2012) 4989.
[24] Buchter A. *et al.*, *Phys. Rev. Lett.*, **111** (2013) 067202.
[25] Landeros P., Allende S., Escrig J., Salcedo E., Altbirm D. and Vogel E. E., *Appl. Phys. Lett.*, **90** (2007) 102501.
[26] Landeros P. and Núñez A. S., *J. Appl. Phys.*, **108** (2010) 033917.
[27] Yan M., Andreas C., Kákay A., García-Sánchez F. and Hertel R., *Appl. Phys. Lett.*, **100** (2012) 252401.
[28] Otálora J. A., López-López J. A., Vargas P. and Landeros P., *Appl. Phys. Lett.*, **100** (2012) 072407.
[29] Otálora J. A., López-López J. A., Landeros P., Vargas P. and Núñez A. S., *J. Magn. & Magn. Mater.*, **341** (2013) 68.
[30] Yan M., Andreas C., Kákay A., García-Sánchez F. and Hertel R., *Appl. Phys. Lett.*, **99** (2011) 122505.
[31] Gou Y., Goussev A., Robbins J. M. and Slastikov V., *Phys. Rev. B*, **84** (2011) 104445.
[32] Aharoni A., *Introduction to the Theory of Ferromagnetism*, 2nd edition (Clarendon Press, Oxford) 2001.
[33] Carbou G., *Math. Models Methods Appl. Sci.*, **11** (2001) 1529.
[34] Kohn R. V. and Slastikov V., *Arch. Ration. Mech. Anal.*, **178** (2005) 227.
[35] Kohn R. V. and Slastikov V., *Proc. R. Soc. A*, **461** (2005) 143.